

# Effect of shape on mechanical properties and deformation behavior of Cu nanowires : An atomistic simulations study

P. Rohith<sup>a,\*</sup>, G. Sainath<sup>b</sup>, V.S. Srinivasan<sup>c,d</sup>

<sup>a</sup>*Nanomechanics Simulations Laboratory, Faculty of Mechanical Engineering, Technion-Israel Institute of Technology, Haifa-320003, Israel*

<sup>b</sup>*Materials Development and Technology Division, Indira Gandhi Centre for Atomic Research, Kalpakkam, Tamilnadu-603102, India*

<sup>c</sup>*Homi Bhabha National Institute (HBNI), Indira Gandhi Centre for Atomic Research, Kalpakkam, Tamilnadu-603102, India*

<sup>d</sup>*Scientific Information Resource Division, Resource Management & Public Awareness Group, Indira Gandhi Centre for Atomic Research, Kalpakkam, Tamilnadu-603102, India*

---

## Abstract

We study the effect of nanowire shape on mechanical properties and deformation behaviour of Cu nanowires using atomistic simulations. Simulations were carried out on [100] nanowires with different shapes such as triangular, square, pentagon, hexagon and circular. Based on size, two different scenarios were considered. In first, all shapes have different surface area to volume ratio, while in second, all have the same surface area to volume ratio. The results indicate that the Young's modulus is insensitive to shape in both cases. However, yield strength is different for different shapes. In both cases, triangular nanowire exhibit the lowest yield strength, while circular nanowire is the strongest. Deformation in all the nanowires is dominated by partial slip and twinning. Due to twinning, different shapes expose different surfaces at the twinned region. All nanowires show ductile failure and square nanowire exhibits the highest failure strain, while it is lowest for triangular nanowire.

*Keywords:* Molecular Dynamics simulations; Cu nanowires; Shape effect; Strength ; Dislocations

---

## 1. Introduction

In recent years, nanowires have been a major focus of scientific research due to their remarkable electrical, magnetic, optical and mechanical properties [1]. These distinct properties of nanowires arise mainly due to their finite size, high surface area to volume ratio and limited defect density [2, 3]. With increasing size, the surface area to volume ratio decreases and becomes negligible for bulk materials. As a result, the size effects are often seen mainly in nanoscale materials. In view of potential applications in nano electro mechanical systems (NEMS), huge research on nanowires has been carried in the past decade to understand the mechanical behaviour under the influence of various parameters [2, 3]. Out of all the parameters, the size of the nanowires has been considered as the most important parameter that influences the mechanical

---

\*Corresponding author

*Email address:* `prohith@campus.technion.ac.il` (P. Rohith)

behaviour of nanowires [2, 3, 4, 5, 6]. It has been reported that the properties such as Young's modulus, yield strength and strain to failure are strongly dependent on nanowire size [2, 3, 7, 8]. With increasing nanowire size, the values of Young's modulus and yield strength first decreases and then saturates towards a constant value [7, 8, 9]. Zhu et al. [9] had performed in-situ tensile testing of Ag nanowires with diameters between 34 and 130 nm. It can be clearly seen from their studies that Young's modulus of nanowires decreases with increasing diameter and finally attains saturation at a magnitude corresponding to the Young's modulus of bulk Ag. Similarly, it has been reported that the yield stress also exhibit a rapid decrease in small size nanowires followed by gradual decrease towards saturation at larger size [7]. Further, the yield stress value at saturation has been found to be close to the theoretical/ideal strength of the nanowire [7]. Along with nanowire size, the other factors such as crystallographic orientation [10, 11, 12], mode of loading [12], strain rate [13], temperature [13, 14, 15] and shape [14, 16, 17] also influences the mechanical behaviour and deformation mechanisms of single crystalline nanowires.

With regard to nanowire shape, Leach et al. [16] had performed the MD simulations on silver nanowires with different cross-sectional geometries such as pentagon, rhombic, and truncated-rhombic. It has been shown that the pentagon shape Ag nanowires exhibit higher strength compared to rhombic and truncated-rhombic shapes. They had also reported that for all the shapes, the yield strength decreases with increasing cross-section width [16]. Similarly, Cao and Ma [14] have shown that the yield stress of circular shaped  $\langle 111 \rangle$  Cu nanowires is about 10 GPa, while for square shaped nanowire 6.5 GPa has been reported as the yield strength. In the literature, it has been found that apart from mechanical properties, the nanowire shape influences many different material properties such as Debye temperature [18], melting mechanisms [19] and absorption[20]. For instance, Arora et al. [18] had studied the role of shape and size on the Debye temperature of Au, Ag, Cu and Co with three different shapes like spherical, tetrahedral and octahedral. They had reported that Debye temperature is maximum for tetragonal shape, and minimum for spherical shape. They had explained this variation on the basis of surface area to volume ratio, which varies with shape and size [18]. The surface area to volume ratio is minimum for spherical shape, while it is maximum for tetragonal [18]. Kateb et al. [19] had reported the differences in melting mechanisms of Pd cub-octahedron and icosahedron structures. They had reported that the large icosahedron structures melts through a combination of surface and diagonal melting. On the other hand, in cub-octahedron structures, surface melting occurred by nucleation of the liquid phase at (100) planes and growth of liquid phase occurs at the surface before inward growth [19]. Using simulation studies, Kadam et al. [20] had studied the optical properties of GaAs quantum dots with different shapes such as cuboid, cylinder, dome, cone, and pyramid. They had suggested that the both cuboid and cylinder shaped quantum dots show maximum absorption, whereas minimum absorption is observed for the dome-shaped quantum dots [20]. All these studies indicate that the shape greatly influences various properties of materials.

As the nanowire shape/geometry influences the surface area to volume ratio, which in turn affects the material properties, the mechanical behaviour of nanowires with different cross-sectional shapes such as

triangular, pentagonal and hexagonal also should be known apart from the well studied square and circular shapes. In this context, it is surprising to find that there is no systematic study in the literature on how the nanowire shape influences the mechanical properties and associated deformation mechanisms of nanowires. Further, the details of twinning related effects such as the orientation of the twinned region and twin growth have not been investigated in nanowire shapes other than square and circular. In view of this backdrop, the present investigation is aimed at understanding the role of nanowire cross-sectional shape on mechanical properties, deformation and failure behaviour of nanowires using atomistic simulations. The tensile loading has been applied on nanowires with different shapes such as triangular, square, pentagonal, hexagonal and circular cross-sections.

## 2. MD Simulation details

The tensile deformation of Cu nanowires with different cross-section shapes have been performed using molecular dynamics (MD) simulations through Large scale Atomic/Molecular Massively Parallel Simulator (LAMMPS) package [21]. In order to specify the atomic description of Cu atoms, an embedded atom method (EAM) potential for FCC Cu given by Mishin and co-workers [22] has been employed in the present study. This potential has been chosen for being able to reproduce the generalized stacking fault and twinning fault energies for Cu [23], which are key variables for predicting the dislocation and plasticity related properties.

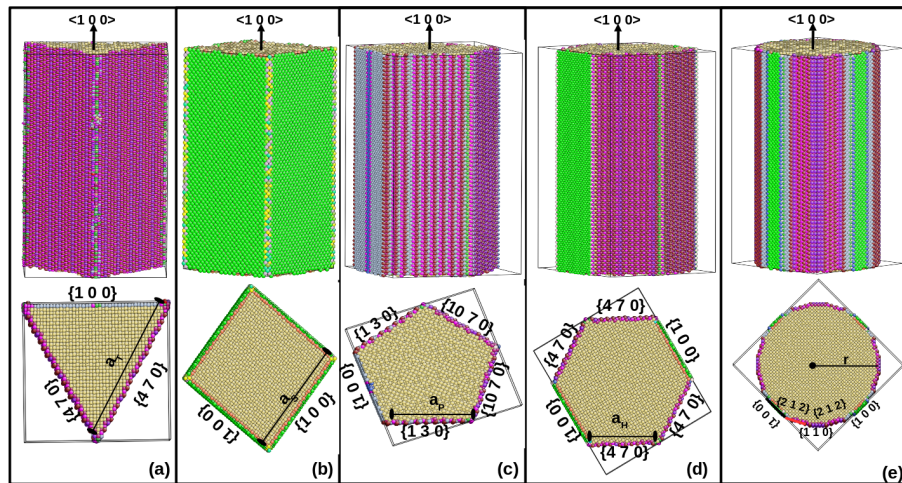


Figure 1: The nanowires cross-section shapes considered in the present study. (a) Triangular, (b) square, (c) pentagonal, (d) hexagonal, and (e) circular, with their corresponding side surfaces.

In order to study the influence of shape of the nanowires, five different cross-sectional geometries i.e., triangle, square, pentagon, hexagon and circle have been chosen in the present study (Figure 1). All the nanowires in the present study were oriented in  $\langle 100 \rangle$  along axial direction enclosed by different surfaces. The equilibrated side surfaces for all nanowires with different cross-sections has been shown in Figure 1. It can be seen that the triangular and hexagonal shaped nanowires have enclosed by  $\{470\}$  and  $\{100\}$  type side surfaces, while square nanowire is enclosed by all  $\{100\}$  type surfaces (Figure 1). Similarly, the pentagonal

shaped nanowire has  $\{130\}$ ,  $\{10\bar{7}0\}$  and  $\{100\}$  as side surfaces, while the circular nanowire is surrounded by  $\{100\}$ ,  $\{110\}$  and  $\{212\}$  type side surfaces (Figure 1). For all the nanowires, periodic boundary conditions have been chosen only along the length direction ( $\langle 100 \rangle$ ), while the other directions were kept free in order to mimic an infinitely long nanowire.

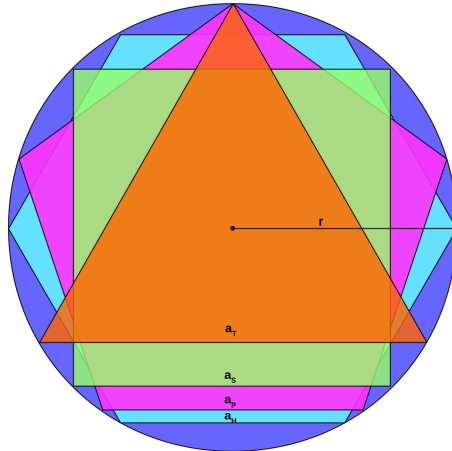


Figure 2: A model system showing the inscription all the shapes within the circular shape. In the first scenario, the size for different shapes is chosen in such a way that all shapes can be inscribed in circular nanowire of radius  $r$ .  $a_T, a_S, a_P$ , and  $a_H$  represents the side length of triangular, square, pentagonal and hexagonal shaped nanowires.

The size of nanowires of different shapes has been chosen in two different ways. In the first scenario, the size of the nanowires of different shapes is chosen in such a way that it can be inscribed in a nanowire with circular cross-section as shown in Figure 2. As a consequence, all shapes have different surface area to volume ratio as shown in Table 1. In the second scenario, the size of the nanowires has been chosen in such a way that the surface area to volume ratio of all the shapes remains constant (Table 2). The corresponding size of nanowires of different shapes is shown in Table 1 and 2 for these two different cases of varying and constant surface area to volume ratios. For both cases, the length of all the nanowires has been chosen as two times that of the cross-section width i.e., an aspect ratio of 2:1.

Table 1: The nanowire size and surface area to volume ratio of different shapes in Scenario-1. In this scenario, the nanowire size has been chosen in such a way that all shapes can be inscribed in circular shape as shown in Figure 2.

Nanowire shape	Side length (a), nm	Surface area to volume ratio
Triangle	8.66	0.8
Square	7.07	0.565
Pentagon	5.88	0.496
Hexagon	5	0.46
Circle	10	0.4

Following the creation of the model nanowires with different shapes, the energy minimization was performed by a conjugate gradient method to obtain a relaxed structure. To retain the sample at the required temperature, all the atoms have been assigned initial velocities according to the Gaussian distribution.

Table 2: The nanowire size and surface area to volume ratio of different shapes in Scenario-2. In this scenario, the nanowire size has been chosen in such a way that all the shapes have same surface area to volume ratio.

Nanowire shape	Side length (a), nm	Surface area to volume ratio
Triangle	17.32	0.4
Square	10	0.4
Pentagon	7.26	0.4
Hexagon	5.77	0.4
Circle	10	0.4

Following this, the nanowires were thermally equilibrated to a required temperature of 10 K in canonical ensemble (constant NVT) with a Nose-Hoover thermostat. The velocity verlet algorithm has been used to integrate the equations of motion with a time step of 2 fs. Following thermal equilibration, the tensile deformation was carried out by maintaining a constant strain rate of  $1 \times 10^8 \text{ s}^{-1}$  along the axial direction. Strain ( $\varepsilon$ ) has been calculated as  $(l - l_0)/l_0$ , where  $l$  is instantaneous length and  $l_0$  is the initial length of the nanowire. The stress has been obtained using the Virial expression [24], which is equivalent to a Cauchy's stress in an average sense. Following the MD simulations, the atomic configuration of nanowires during the deformation has been visualized using AtomEye package [25]. Common neighbour analysis (CNA) [26, 27] has been used to identify the stacking faults.

### 3. Results

The effect of shape on the mechanical properties and deformation behaviour of nanowires has been studied for two different scenarios. In the first scenario, the nanowires having different shapes leading to different surface area to volume ratio have been chosen (Table 1), while in the second scenario, all the nanowires of different shapes have a same surface area to volume ratio (Table 2). The results for these two different cases are presented in the following;

#### 3.1. Nanowires of different shape having different surface area to volume ratio

In this scenario, the size of the nanowires of different shapes has been chosen in such a way that all the shapes can be inscribed in nanowire of circular cross-section shape having diameter of 10 nm (Figure 2). Accordingly, all nanowires have different surface area to volume ratio (Table 1). The circular nanowire has a lowest surface area to volume ratio of 0.4, while the triangular nanowire has the highest and twice the value of circular nanowire. Figure 3 shows the stress-strain behaviour of nanowires of different shape having different surface area to volume ratio. For better clarity, inset figure shows the stress-strain curve till a strain value of 20%. Initially, all the nanowires show linear elastic behaviour up to a peak value followed by an abrupt drop in flow stress (except triangular nanowire). In triangular nanowire, the abrupt drop in flow stress is absent and flow stress increases marginally after yielding to a peak value of 5.16 GPa. Following

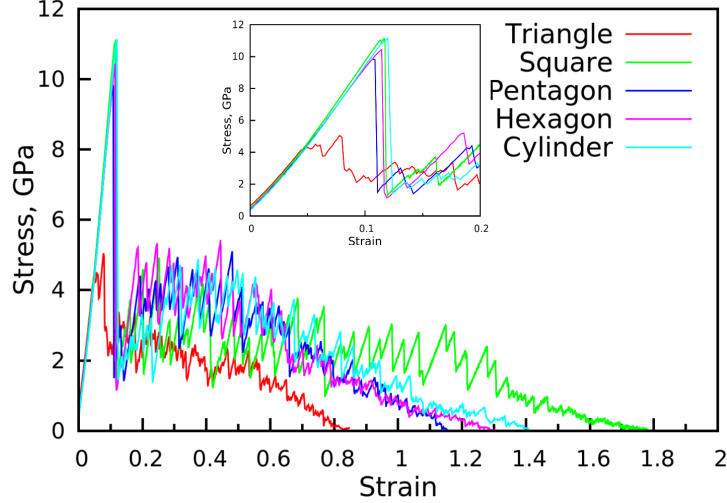


Figure 3: Stress-strain behaviour of  $\langle 100 \rangle$  Cu nanowires of different shape in Scenario-1, where each shape has a different surface area to volume ratio. The stress-strain behaviour till strain of 20 % has been shown in inset for better clarity.

the yielding in all the nanowires, the flow stress decreases continuously with increase in strain till failure. During this decrease, the flow stress exhibits a rapid fluctuations (Figure 3). Further, the flow stress of the triangular nanowires is always lower than the flow stress of the other nanowires. Finally, the square shaped nanowire exhibits the highest failure strain of around 180%, while the failure strain is lowest for triangular shaped nanowire.

Figure 3 also shows that the slope of linear elastic regime is almost same for all the nanowires, which indicates that the Young's modulus is insensitive to the nanowire shape. The value of Young's modulus is obtained as 92 GPa, which is in good agreement with previous reported value [28]. Further, in the atomistic simulation study of Cao and Ma [14], it was observed that both circular and square shaped nanowires possess the same value of Young's modulus, which affirm the present observation that the Young's modulus is insensitive to nanowire shape. Here, it is interesting to see that despite the different surface area to volume ratio, Young's modulus remains same for different shapes. However, it must be noted that Young's modulus can be influenced by surface area to volume ratio when it is varied by nanowire size [7, 8, 28]. The variations in yield strength for nanowires of different shapes has been presented in Figure 4. It can be seen that the triangular nanowires exhibits a minimum yield strength value of 5.16 GPa. The magnitude of yield strength increases with increasing the number of the side surfaces and attains a maximum for circular shaped nanowire (Figure 4). The variations in yield stress values for different shapes can be attributed to the variations in surface area to volume ratio. The surface area to volume ratio for different shapes has been calculated (Table 1) and plotted by superimposing in Figure 4. It can be seen that the surface area to volume ratio decreases in the order of triangular, pentagonal, hexagonal, and circular nanowires. These variations clearly indicates that yield stress is inversely proportional to surface area to volume ratio, i.e., the yield strength of nanowires is high for nanowires with low surface area to volume ratios (Figure 4).

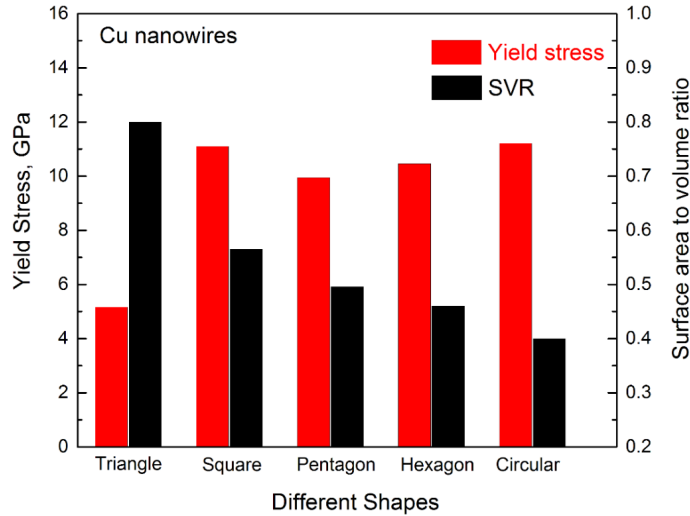


Figure 4: Variation of yield strength along with surface area to volume ratio for different nanowire shapes in Scenario-1.

### 3.2. Nanowires of different shapes having same surface area to volume ratio

In previous section, the effect of shape has been studied by considering different nanowire shapes having different surface area to volume ratio. In order to study the sole effect of shape, here the surface area to volume ratio has been kept same for all shapes. Accordingly, the size of the nanowires has been varied as shown in Table. 2. Figure 5 shows the stress-strain behaviour of nanowires of different shapes with same surface area to volume ratio under tensile loading. For clarity, the magnified version of stress-strain behaviour till a strain value of 20 % has been shown in inset figure. Similar to scenario-1, all the nanowires exhibit linear elastic deformation up to a peak value of stress. After elastic deformation, all the nanowires including the triangular one show a drastic yield drop followed by decrease in flow stress with increasing strain until failure. Further, as in the previous case, the flow stress of the triangular nanowires is considerably lower than the flow stress of the other nanowires (Figure 5). Finally, the square shaped nanowire exhibits the highest failure strain, while it is lowest for hexagon and triangular shaped nanowires (Figure 5).

Similar to previous scenario, the Young's modulus has been calculated as the slope of the linear elastic regime and found to be around 92 GPa for all nanowires. This indicate that the Young's modulus is insensitive to the nanowire shape, irrespective of whether the surface area to volume ratio is varied or kept constant. The variations in yield stress for different shaped nanowires with same surface area to volume ratio is shown in Figure 6. Here, it is interesting to observe that despite the same surface area to volume ratio, the yield strength still varies for different shapes. Like the previous scenario, the triangular nanowire exhibits the lowest yield stress and it increases with increasing number of side surfaces before attaining the maximum for circular nanowire. However, unlike the previous case, this variation in yield stress cannot be explained by the surface area to volume ratio as it is constant. To understand this variations in the present scenario, the potential energy for different shapes has been calculated and shown in Figure 6. Interestingly,

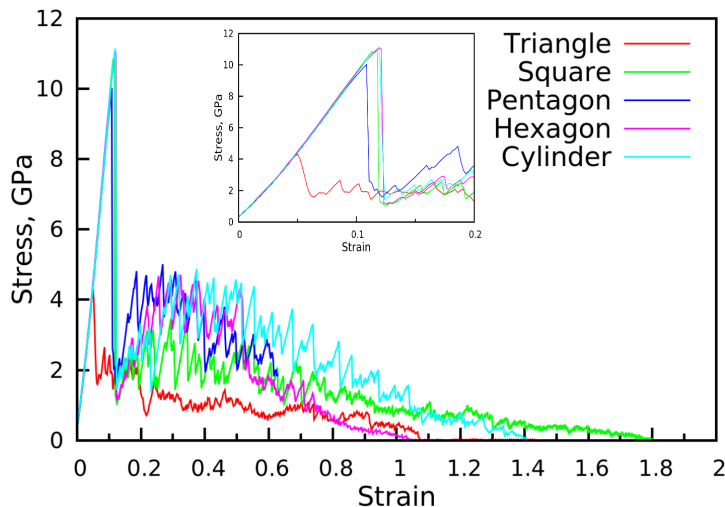


Figure 5: Stress-strain behaviour of  $\langle 100 \rangle$  Cu nanowires of different shape in Scenario-2, where all the shapes have same surface area to volume ratio. The stress-strain behaviour till strain of 20 % has been shown in inset for better clarity.

both the potential energy and yield stress varies in a similar fashion. Like yield stress, the potential energy also increases with increase in number of side surfaces exhibiting the highest value for circular nanowire and the lowest for triangular nanowire. These variations indicates that there exists a one to one correlation between potential energy and yield stress. Hence, the variations in yield strength can be attributed to the variations in potential energy of the nanowires (Figure 6). Here, it must be noted that in the previous case (nanowires with different shape and different surface area to volume ratio), there were no significant variations in potential energy and no correlation has been found between yield stress and potential energy.

#### 4. Deformation behaviour

In order to understand the effect of shape on the dislocation nucleation and deformation mechanisms, the atomic configurations have been analysed for two different scenarios using the CNA parameter and visualized using AtomEye. The results indicate that the defect nucleation and deformation mechanisms were same for both the scenarios. Following yielding, the sudden drop in flow stress corresponds to the defect nucleation in the nanowires and this can also be considered as the initiation of plastic deformation. The initial defect nucleation corresponding to the yielding in the nanowires of different shapes is shown in Figure 7. It can be seen that in all the nanowires including the circular one, the yielding occurs through the nucleation of  $1/6\langle 112 \rangle$  Shockley partial dislocations from the corners (or intersection of two different side surfaces) of the nanowires. In circular nanowire, the defect nucleation has been observed from the intersection of  $\{212\}$  and  $\{110\}$  type side surfaces (Figure 2). It is well known that the atoms at the corners (or intersection of two different side surfaces) of nanowires have low coordination resulting in high stress concentration. As a result, the corners act as a favourable sites for defect nucleation (Figure 7).

Following the nucleation of Shockley partials from the corners, the deformation behaviour in nanowires of different shapes is dominated by the slip through partial dislocations along with deformation twinning

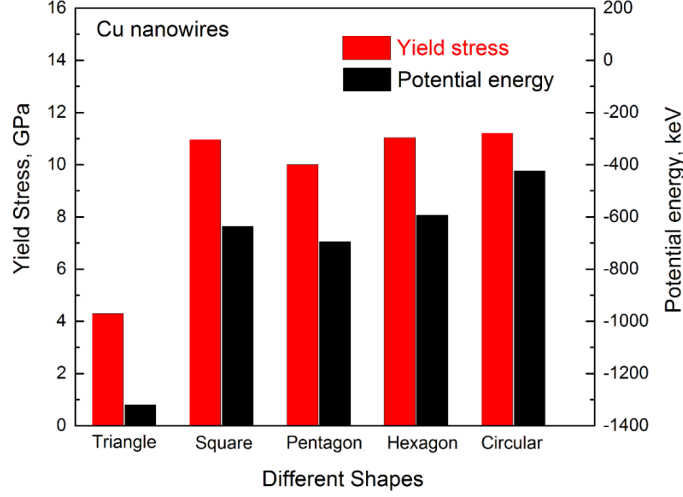


Figure 6: Variation of yield strength and potential energy for different nanowire shapes in Scenario-2.

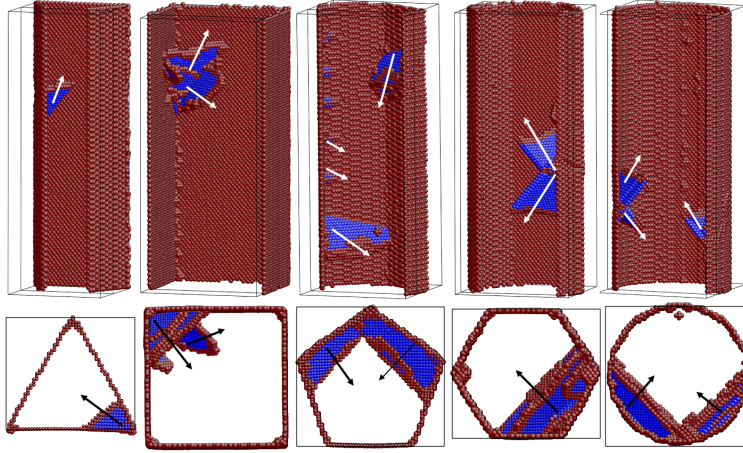


Figure 7: The dislocation nucleation during the yielding/beginning of plastic deformation in nanowires of different shapes. This nucleation mechanism remains the same for both scenarios. The white arrows indicates the direction of dislocation motion. The nucleation occurs from the intersection of two different side surfaces.

(Figure 8). However, occasionally the extended dislocations were also observed, but only at high strains ( $> 50\%$ ). As shown in Figure 8, the twinning has been observed on multiple  $\{111\}$  planes. It has been well known that the deformation twinning alters the surface orientation of the nanowires at the twinned region [10, 11, 12, 29]. In the present study, the deformation twinning changed the initial  $\{100\}$  side surface of square shaped nanowires to  $\{111\}$  type surface (Figure 9b). Similarly, in triangular and hexagonal shaped nanowires, the twinning changes the initial  $\{470\}$  surface to  $\{315\}$  type surface and  $\{100\}$  surface to  $\{111\}$  surface (Figure 9a & c). In pentagonal and circular nanowires, eventhough the deformation twinning has been observed, but we are not able to identify the new surface orientations due to high roughness.

Figure 10 shows the necking and final failure behaviour in nanowires with different cross-section shapes. As shown in Figure 8, the plastic deformation spreads across the nanowire length. Following uniform deformation, the discrete dislocation interactions among different partials leads to the formation of a localized

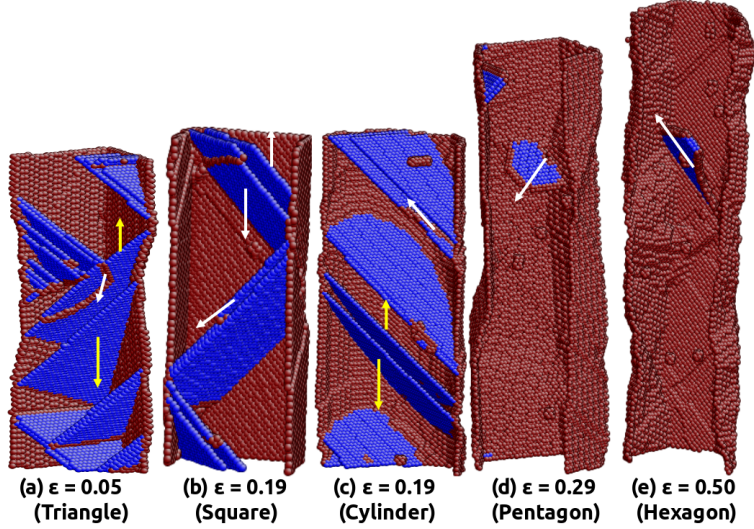


Figure 8: The deformation mechanisms observed in nanowires of different shapes, each shown at different strain value. The yellow arrows indicate the direction of twin boundaries movement. The white arrows indicate the direction of glide of Shockley partial dislocations on  $\{111\}$  planes.

necking (Figure 10). In all nanowires, like dislocation nucleation, the necking starts from the corners or the intersection of different side surfaces of the nanowires (Figure 10). The formation of necking localizes the plastic deformation and also minimize the effect of corners for any further dislocation nucleation. The localized plastic deformation results in final failure of the nanowires in a ductile manner (Figure 10).

In single crystal nanowires, the deformation by partial or full dislocation slip can be understood based on the parameter  $\alpha_M$ , defined as the ratio of Schmid factors for leading and trailing partial dislocations [12, 30]. For a given orientation of a nanowire, if  $\alpha_M > 1$ , the deformation by twinning/partial dislocation slip is favoured. On the other hand, if  $\alpha_M < 1$ , the deformation by full/extended dislocations is favoured. Similarly, if  $\alpha_M = 1$ , the deformation can proceed either through twinning or extended dislocations or by the combination of these two. It has been shown that for  $\langle 100 \rangle$  orientation, the value of  $\alpha_M$  is 0.5 under tensile loading [12]. Accordingly, the deformation by full/extended dislocation should be observed. However, in the present study the deformation through slip of Shockley partials has been observed (Figure 8). This discrepancy between the predicted and observed deformation mechanism can be attributed to the effects associated with side surfaces [10, 11], whose contribution is absent in the analysis based on  $\alpha_M$ . Similar to the present study, many previous studies [10, 11] have shown that the nanowires oriented  $\langle 100 \rangle$  tensile axis deform by partial dislocation slip under tensile loading.

## 5. Conclusions

Molecular dynamics simulations have been performed to understand the influence of nanowire shape on the mechanical properties and the deformation mechanisms of Cu nanowires. Five different shapes (triangular, square, pentagon, hexagonal and circular) have been considered. Based on nanowires size, two different scenarios have been chosen. In the first scenario, the size of the nanowires has been chosen in such

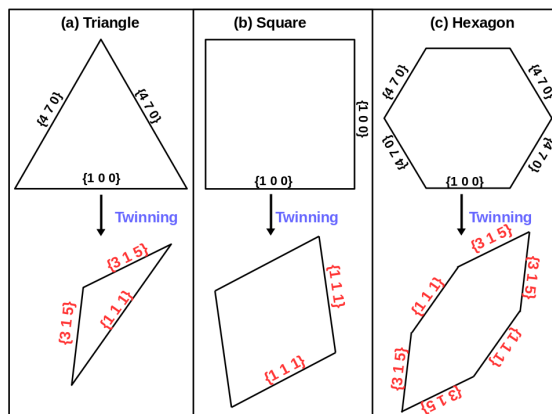


Figure 9: The schematic showing the orientation of initial (top row) and twinned side surfaces for (a) triangular, (b) square and, (c) hexagonal shaped nanowires. In pentagonal and circular nanowires, even though the deformation twinning has been observed, but we are not able to identify the new surface orientations due to high roughness.

a way that all the shapes can be inscribed in nanowire of circular cross-section with a diameter 10 nm. In this case, all nanowires possess different surface area to volume ratios. In the second scenario, the size of the nanowires has been chosen in such a way that the surface area to volume ratio remains same for all shapes. The MD simulations results indicate that the Young's modulus in both scenarios is insensitive to the nanowire shape. This insensitivity of Young's modulus is interesting particularly in first scenario, where different shapes have different surface area to volume ratio. In both the scenarios, the yield strength increases with increasing number of side surfaces. The traingular nanowire shows the lowest strength and ductility (failure strain), while the circular nanowire display highest strength combined with good ductility. Here, it is interesting to observe that despite the same surface area to volume ratio in the second scenario, the yield strength still varies for different shapes. The variations in yield strength have been explained based on the variations in surface area to volume ratio (First scenario) and potential energy (Second scenario) of the nanowires. In all the nanowires, irrespective of their shape and surface area to volume ratio, the deformation is dominated by the slip through Shockley partial dislocations and deformation twinning. The deformation twinning changed the orientation of side surfaces at the twinned region, whose orientation is different for different shapes. Finally nanowires of all shapes fail in a ductile manner.

## References

## References

- [1] C.M. Lieber, Nanoscale science and technology: Building a big future from small things, MRS Bull. 28 (2003) 486.
- [2] Y. Chen, X. An, and X. Liao, Mechanical behaviors of nanowires, Appl. Phys. Rev. 4 (2017) 031104.
- [3] S. Wang, Z. Shan, and H. Huang, The mechanical properties of nanowires, Adv. Sci. 4 (2017) 1600332.

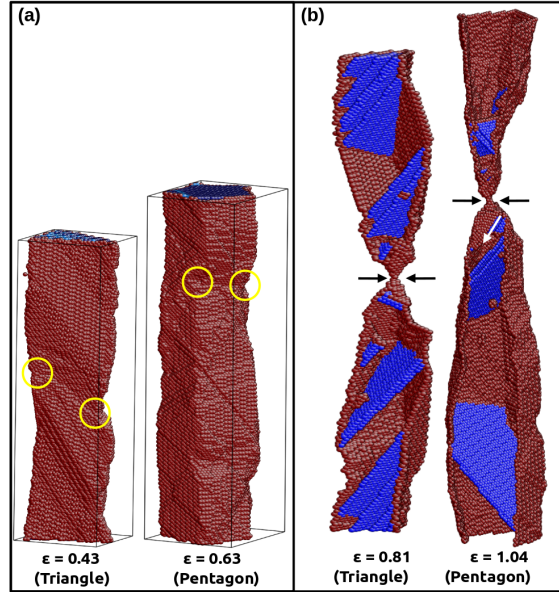


Figure 10: The final failure behaviour of nanowires of different shapes. The encircled regions indicate the initiation of necking and black arrows show failed region.

- [4] M.D. Uchic, D.M. Dimiduk, J. N. Florando, W.D. Nix, Sample dimensions influence strength and crystal plasticity, *Science* 305 (2004) 986.
- [5] C. Peng, Y. Zhan, J. Lou, Size-dependent fracture mode transition in copper nanowires, *Small* 8 (2012) 1889.
- [6] M. Yaghoobi, G.Z. Voyiadjis, Size effects in fcc crystals during the high rate compression test, *Acta Mater.* 121 (2016) 190.
- [7] G. Sainath, P. Rohith, B.K. Choudhary, Size dependent deformation behaviour and dislocation mechanisms in  $\langle 100 \rangle$  Cu nanowires, *Philos. Mag.* 97 (2017) 2632.
- [8] P. Rohith, G. Sainath, B.K. Choudhary, Molecular dynamics simulation studies on the influence of aspect ratio on tensile deformation and failure behaviour of  $\langle 100 \rangle$  copper nanowires, *Comp. Mater. Sci.* 138 (2017) 34.
- [9] Y. Zhu, Q. Qin, F. Xu, F. Fan, Y. Ding, T. Zhang, B. J. Wiley, and Z.L. Wang, Size effects on elasticity, yielding, and fracture of silver nanowires: In situ experiments, *Phys. Rev. B* 85 (2012) 045443.
- [10] H.S. Park, K. Gall, J.A. Zimmerman, Deformation of FCC nanowires by twinning and slip *J. Mech. Phys. Solids* 54 (2006) 1862.
- [11] C.R. Weinberger and W. Cai, Plasticity of metal nanowires, *J. Mater. Chem.* 22 (2012) 3277.
- [12] P. Rohith, G. Sainath, B.K. Choudhary, Effect of orientation and mode of loading on deformation behaviour of Cu nanowires *Comp. Condens. Mat.* 17 (2008) e00330.

- [13] H. Xie, F. Yin, T. Yu, G. Lu, Y. Zhang, A new strain-rate-induced deformation mechanism of Cu nanowire: Transition from dislocation nucleation to phase transformation, *Acta Mater.* 85 (2015) 191.
- [14] A. Cao, E. Ma, Sample shape and temperature strongly influence the yield strength of metallic nanopillars. *Acta Mater.* 56 (2008) 4816.
- [15] G. Sainath, B. K. Choudhary, Atomistic simulations on ductile-brittle transition in  $\langle 111 \rangle$  BCC Fe nanowires, *J. Appl. Phys.* 122 (2017) 095101.
- [16] A.M. Leach, M. McDowell, K. Gall, Deformation of top-down and bottom-up silver nanowires, *Adv. Funct. Mater.* 17 (2007) 43.
- [17] Y. Zhang, H. Huang, Do Twin Boundaries Always Strengthen Metal Nanowires?, *Nano Res. Lett.* 4 (2009) 34.
- [18] N. Arora, D. P. Joshi, P. Uma, Size and shape dependent Debye temperature of nanomaterials. *Mater. Today Proc.* 4 (2017) 10450.
- [19] M. Kateb, M. Azadeh, P. Marashi, S. Ingvarsson, Size and shape-dependent melting mechanism of Pd nanoparticles, *J. Nanopart. Res.* 20 (2018) 251.
- [20] K.D. Kadam, S.L. Patil, H.S. Patil, P.P. Waifalkar, K.V. More, R.K. Kamat, T.D. Dongale, Shape dependent optical properties of GaAs quantum dot: A simulation study, *J. Nano Electr. Phys.* 11 (2019) 01013.
- [21] S. Plimpton, Fast parallel algorithms for short-range molecular dynamics, *J. Comp. Phys.* 117 (1995) 1.
- [22] Y. Mishin, M.J. Mehl, D.A. Papaconstantopoulos, A.F. Voter, J.D. Kress, Structural stability and lattice defects in copper: Ab initio, tight-binding, and embedded-atom calculations, *Phys. Rev. B*, 63 (2001) 1.
- [23] W. Liang, M. Zhou, Atomistic simulations reveal shape memory of fcc metal nanowires, *Phys. Rev. B* 73 (2006) 115409.
- [24] J.A. Zimmerman, E.B. Webb, J.J. Hoyt, R.E. Jones, P.A. Klein, D.J. Bammann, Calculation of stress in atomistic simulations, *Modell. Simul. Mater. Sci. Eng.* 12 (2003) S319.
- [25] J. Li, AtomEye: an efficient atomistic configuration viewer, *Modell. Simul. Mater. Sci. Eng.* 11 (2003) 173.
- [26] D. Faken, H. Jonsson, Systematic analysis of local atomic structure combined with 3D computer graphics, *Comp. Mater. Sci.* 2 (1994) 279.
- [27] H. Tsuzuki, P.S. Branicio, J.P. Rino, Structural characterization of deformed crystals by analysis of common atomic neighborhood, *Comp. Phys. Comm.* 177 (2007) 518.

- [28] H. Liang, M. Upmanyu, H. Huang, Size-dependent elasticity of nanowires: Nonlinear effects, *Phys. Rev. B* 71 (2005) 241403 (R).
- [29] J. Diao, K. Gall, M.L. Dunn, Surface stress driven reorientation of gold nanowires, *Phys. Rev. B* 70 (2004) 075413.
- [30] Z.J. Wang, Q.J. Li, Y. Li, L.C. Huang, L. Lu, M. Dao, J. Li, S. Suresh, Z.W. Shan, Sliding of coherent twin boundaries, *Nat. Commun.* 8 (2017) 1108.